

Long-Term Assessment of the Reflectivity Biases and Wet-Radome Effect in Operational S-band Dual-Polarimetric Radar in northern Taiwan

Jui Le Loh¹, Pin-Fang Lin², Wei-Yu Chang¹, Pao-Liang Chang², Hsiu-Wei Hsu¹, and Yu-Chieng Liou¹

¹Department of Atmospheric Sciences, National Central University, Jhongli City, Taiwan

²Central Weather Bureau, Taipei, Taiwan

Abstract

The long-term assessment of reflectivity (Z_{HH}) biases using a S-band dual-polarimetric radar (RCWF), operated by the Central Weather Bureau (CWB) of Taiwan (121.77 °E, 25.07 °N) was analyzed in this study. The biases including systematic bias and wet-radome effect (WRE) along with attenuation effect from RCWF were investigated. The differential phase (Φ_{DP}) based attenuation correction ($A_{HH} = \alpha\Delta\Phi_{DP}$ and $A_{DP} = \beta\Delta\Phi_{DP}$) and self-consistency ($K_{DP} = \alpha Z_{HH}^b$) algorithms were applied to estimate the attenuation effect, system bias and WRE of RCWF. The corresponding coefficients of α , β , a , and b were obtained from 11 years of Joss-Waldvogel disdrometer (JWD) data in northern Taiwan. The attenuation and bias calculations due to the uncertainty of coefficients associated with seasonal and temperature variabilities of raindrop size distribution were examined by a series of sensitivity test. The quality of the measurements from RCWF is improved after applied the attenuation and self-consistent methods. The results indicate that RCWF has a consistent systematic bias (~ -2 dB). The WRE period identified by near radar reflectivity (Z_{NR} , mean reflectivity derived within the radar radius of 10 km) showed that additional underestimations in Z_{HH} up to 6 dB can be found in RCWF. In this study, a fitted quadratic polynomial equation is proposed to investigate the estimation of system bias and WRE. This quadratic polynomial equation has shown can simultaneously obtain the systematic biases and WRE using Z_{NR} .

Key words: systematic biases; wet-radome effect; attenuation; self-consistency

1. Introduction

In Taiwan, the property and life lost due to heavy precipitation induced disasters have been an important task for various government agencies. It is essential to mitigate these lost by monitor precipitation systems in real-time. To achieve that, the meteorological radar is the most suitable observation due to its high spatiotemporal resolution. The radar measurements can be used to monitor precipitation systems and estimate the rainfall rate. However, the measurements of radar contain errors such as non-meteorological echoes, bright band contamination, calibration biases of reflectivity (Z_{HH}) and differential reflectivity (Z_{DR}), and others (Kwon et al. 2015). Past studies have been shown that the radar measurement may degrade by the attenuation, system bias, and wet-radome effect (WRE). For examples, Vivekanandan et al. (2003) indicated that 1

dB bias in Z_{HH} produces 18% bias in Z_{HH} -rainfall rate (R) relation for the case of the NEXRAD.

This problem can be solved by different methods depending on the type of measurements involved. The correction for the attenuation effects of radar reflectivity to avoid underestimation of precipitation has been recognized for a long time, especially for C-band radars (Ryde 1946; Atlas and Banks 1951; Hitschfeld and Bordan 1954; Gunn and East 1954; Gorgucci et al. 1996; Carey et al. 2000; Berne 2005). Hitschfeld and Bordan (1954) used the reflectivity measurements made at all the preceding $n-1$ gates, beginning with the gate closest to the radar to correct the attenuation bias at the n^{th} gate. Aydin et al. (1989) introduced a procedure of attenuation correction through the specific horizontal reflectivity (A_{HH} , dB km⁻¹) based on Z_{HH} and Z_{DR} . They noted this procedure was less sensitive to

variations in the drop size distribution (DSD) than past relationships relying on Z_{HH} alone. Gorgucci et al. (1996, 1998) modified and extended this procedure to include a correction at C-band radar for the differential attenuation ($A_{DP} = A_{HH} - A_{VV}$, dB) through a rain medium, where A_{HH} and A_{VV} are the attenuations at horizontal and vertical polarizations, respectively.

Holt (1988) and Bringi et al. (1990) introduced an alternative attenuation correction procedure based on the relationship between the specific differential phase (K_{DP}) and A_{HH}/A_{DP} . They used an estimated differential propagation phase (Φ_{DP}) to correct the Z_{HH} (Z_{DR}) for the deleterious effects of A_{HH} (A_{DP}). This approach has two distinct advantages: 1) Φ_{DP} is unaffected by attenuation as long as the returned power is above the power of noise and 2) Φ_{DP} is independent of radar calibration errors (e.g., Zrnić and Ryzhkov 1996). Keenan et al. (2001) presented that the estimation of attenuation and differential attenuation based on K_{DP} is a function of the relationship between the assumed drop size and shape. The effects of propagation are very sensitive to the assumptions in the analytical parameterization of the large drop tail and existence of the large drops, at C-band radar. According to Goddard et al. (1994) and Scarchilli et al. (1996), self-consistency can be used for radar system calibration among Z_{HH} , Z_{DR} , and Φ_{DP} .

Bringi et al. (2001) were proposed and evaluated a self-consistent and constraint-based algorithm for the sensitivity of the scale factor between K_{DP} and A_{HH}/A_{DP} to both temperature and DSD. This principle has been proven as a robust tool and nowadays widely applied for the attenuation and system bias correction (e.g., Goddard et al. 1994; Scarchilli et al. 1996; Bringi et al. 2001; Vivekanandan et al. 2003; Ryzhkov et al. 2005; Park et al. 2005; Gorgucci and Baldini 2007; Kim et al. 2008, 2010; Kwon et al. 2015; Oh et al. 2016). Gorgucci and Baldini (2007) corrected Z_{HH} and Z_{DR} based on this principle using C-band profiles generated from S-band radar measurements collected by the NCAR S-Pol radar during the Teflun B campaign and C-band radar data

collected by the Polar 55C radar over the region of Rome, Italy. Chen et al. (2017) also used this technique for the attenuation and system bias correction using S-band dual-polarization radar (RCWF) and National Central University (NCU) C-band polarimetric radars data from 2014 to 2015 over northern Taiwan. Hence, it is essential to develop the algorithms to quality control (QC) and utilize all of the data.

The purpose of this study is to analyze the long-term assessment of Z_{HH} biases from an operational S-band dual-polarization radar by accurately calibrating the Z_{HH} and Z_{DR} measurements. The characteristics of RCWF and disdrometer data and the QC procedures are described in Section 2. Next, the results of the long-term monitoring of calibration biases are shown in Section 3.

2. Data and Methods

a. Datasets

The RCWF data were collected from January to December 2017 at Wufenshan, northern Taiwan (121.77 ° E, 25.07 ° N), shown in Fig. 1, operated by the Central Weather Bureau (CWB). The RCWF data were updated every ~6 minutes with 9 elevation angles (0.48°, 1.45°, 2.42°, 3.39°, 4.31°, 6.02°, 9.89°, 14.59°, and 19.5°). The specifications of RCWF are summarized in Table 1. RCWF data are separated into seven different precipitation types, namely all, winter, spring, mei-yu, summer, typhoon, and autumn in 2017. Besides, the Joss-Waldvogel disdrometer (JWD) data from NCU, northern Taiwan (121.17 ° E, 24.97 ° N) were also continuously collected from 2005 to 2015 (Fig. 1) and used to determine the coefficients of α , β , a , and b (derived from A_{HH} , A_{DP} , $\Delta\Phi_{DP}$, K_{DP} , Z_{HH} , and Z_{DR}).

Table 1. Specification of RCWF radar at Wufenshan site.

Radar (Type)	RCWF (WSR-88D)		
Locations	Longitude	Latitude	Altitude
	121.77 °E	25.07 °N	766 m
Wavelength	10.5 cm		
Radial resolution	250 m		
Beam resolution	720		

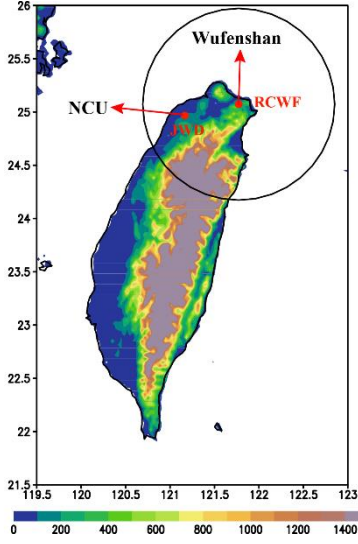


Fig. 1. Geographical locations of RCWF and JWD, which are located at the Wufenshan and National NCU, respectively, in northern Taiwan. The elevation is in meters.

b. Dual-Polarimetric Radar Data Processing

The Tropical Rainfall Measuring Mission (TRMM) Radar Software Library (RSL) was used for converting the raw NEXRAD data to radar universal format (UF) format for RCWF. The Z_{HH} and Z_{DR} bias correction schemes of RCWF was performed as shown in Fig. 2, which included (A) removal of non-meteorological signals, (B) Φ_{DP} processing for noise removal and calculation of $\Delta\Phi_{DP}$, (C) the attenuation correction of Z_{HH} and Z_{DR} , and (D) the WRE and biases correction of Z_{HH} based on self-consistent method.

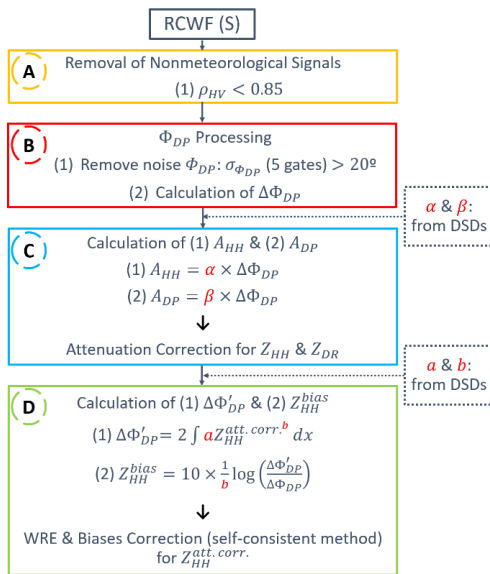


Fig. 2. The QC flowchart for the attenuation, WRE, and systematic biases correction.

A) Removal of Non-meteorological Signals

The basic and simple quality control (QC) to remove noise and non-meteorological signals was performed as part A in Fig. 2. Generally, the value of co-polar correlation coefficient (ρ_{HV}) in rainfall is $\sim 0.98-1$ with the similar raindrop sizes (Liu et al. 1994; Tang et al. 2014; Keat et al. 2016) and yielding values less than 0.75 to identify nonuniform scatters (Park et al. 2009). The non-meteorological signals of RCWF data were removed when $\rho_{HV} < 0.85$.

B) Φ_{DP} Processing

Next, a simple noise removal based on Φ_{DP} was applied as shown in part B of Fig. 2. Firstly, the standard deviation of Φ_{DP} ($\sigma_{\Phi_{DP}}$) of RCWF data was calculated by using five gates centered on the target gate and eliminate it as noise if $\sigma_{\Phi_{DP}} > 20^\circ$. Lastly, the values of $\Delta\Phi_{DP}$ of RCWF data were computed for the attenuation correction of Z_{HH} and Z_{DR} .

C) Attenuation Correction Schemes

Generally, the measurements of Z_{HH} (in $\text{mm}^6 \text{m}^{-3}$) and Z_{DR} are underestimated due to rain attenuation (Chang et al. 2014). Hence, the attenuated measurements of RCWF must be corrected before utilize for other applications or analysis. The calculation of A_{HH} (dB) and A_{DP} (dB) was based on the relation with $\Delta\Phi_{DP}$ ($\Delta\Phi_{DP}$ is twice the sum of K_{DP} over a specified range) as shown in part C of Fig. 2:

$$A_{HH} = \alpha \times \Delta\Phi_{DP} \quad (1)$$

$$A_{DP} = \beta \times \Delta\Phi_{DP} \quad (2)$$

(Bringi et al. 1990; Chang et al. 2014), where α and β were obtained by the linear regression algorithm through the JWD data from NCU. The α and β values were optimized in predetermined bound ranges (in α_{min} , $\alpha_{max} / \beta_{min}$, β_{max}) based on the relations between A_{HH}/A_{DP} and K_{DP} (as shown in eqs. (1) and (2)). The coefficients of α and β used in this study are 0.0197 and 0.0023, respectively with the mean temperature of 20°C .

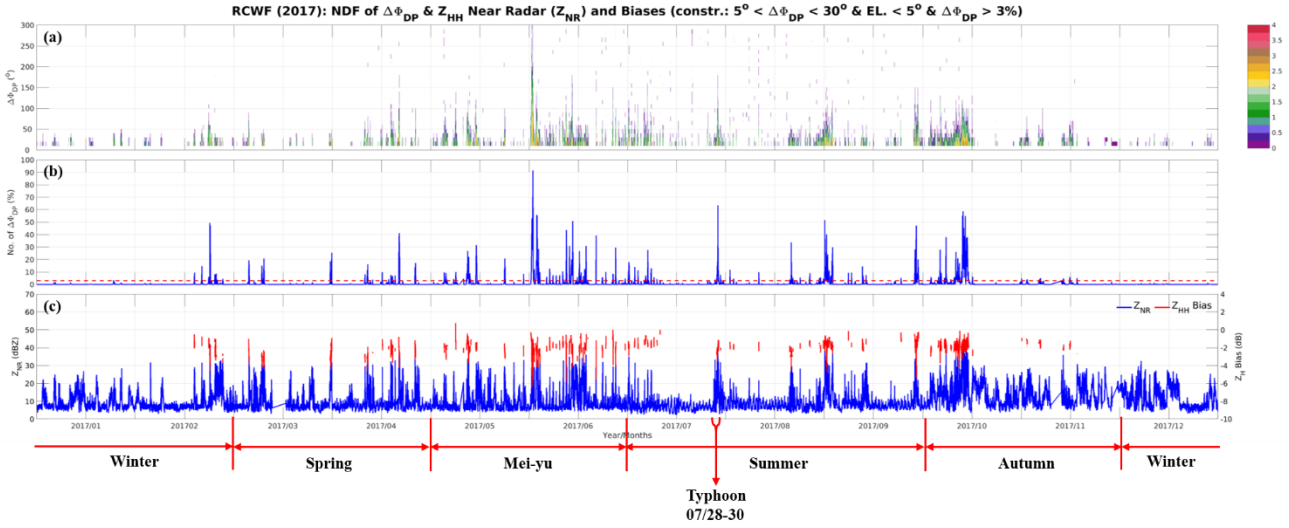


Fig. 3. Time series of (a) the number density distribution of the observed $\Delta\Phi_{DP}$, (b) the percentages of the $\Delta\Phi_{DP}$ data that available (rainy), and (c) Z_{HH} near radar (Z_{NR} , blue line) and biases (red lines; with the constraints that (1) $5^\circ < \Delta\Phi_{DP} < 30^\circ$, (2) elevation angles (EL) $< 5^\circ$, and (3) the percentages of the $\Delta\Phi_{DP} > 3\%$, where the dotted red line as shown in (b)) of RCWF in 2017.

Finally, the observed Z_{HH} (Z_{HH}^{obs}) and Z_{DR} (Z_{DR}^{obs}) can be corrected as following:

$$Z_{HH}^{att. corr.} = Z_{HH}^{obs} + A_{HH} \quad (3)$$

$$Z_{DR}^{att. corr.} = Z_{DR}^{obs} + A_{DP} \quad (4)$$

D) WRE and Biases Correction Schemes

Z_{HH} are dominantly affected by system bias of the radars, WRE, and also attenuation effect. Therefore, the WRE and biases correction of Z_{HH}^{obs} is needed after applied the attenuation correction schemes, based on the $Z_{HH} - K_{DP}$ ($K_{DP} = aZ_{HH}^{att. corr. b}$) self-consistency relationship, as shown in part D of Fig. 2. The calculated $\Delta\Phi_{DP}$ ($\Delta\Phi'_{DP}$) and biases (Z_{HH}^{bias}) can be obtained as following:

$$\Delta\Phi'_{DP} = 2 \int aZ_{HH}^{att. corr. b} dx \quad (5)$$

$$Z_{HH}^{bias} = 10 \times \frac{1}{b} \log \left(\frac{\Delta\Phi'_{DP}}{\Delta\Phi_{DP}} \right) \quad (6)$$

where a and b are 5.52×10^{-5} and 0.8940, respectively, obtained by the linear regression algorithm through the JWD data from NCU. Finally, the true values of Z_{HH}^{obs} (Z_{HH}^{true}) can be obtained as follows:

$$Z_{HH}^{true} = Z_{HH}^{att. corr.} + Z_{HH}^{bias} \quad (7)$$

3. Results and Discussions

Fig. 3 shows a time series of the number density distribution of the observed $\Delta\Phi_{DP}$, the percentages of the $\Delta\Phi_{DP}$ data that available, and Z_{HH} near radar (Z_{NR} , mean reflectivity derived within the radar radius of 10 km) of RCWF in 2017. The mean Z_{HH} biases vary from -6.33 to 0.75 dB, with the constraints of observed $\Delta\Phi_{DP}$, elevation angles, and the data volume coverage. Besides, the attenuation and biases calculations due to the data volume coverage were also examined by a series of sensitivity test as shown in Fig. 4 and Fig. 5. Fig. 4 presents a probability density function (PDF) of the biases in different constraints. The peak of the mean biases with constraints of the observed $\Delta\Phi_{DP}$, elevation angles, and Z_{NR} (red line) is more concentrated than the others.

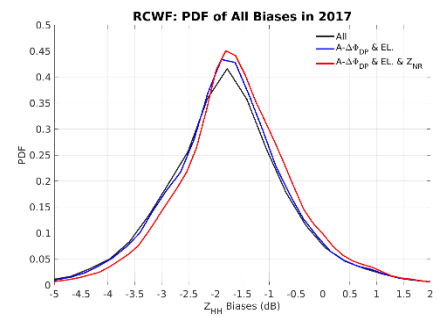


Fig. 4. The probability density function (PDF) of the averaged biases with or without constraints of observed $\Delta\Phi_{DP}$, EL, and Z_{NR} .

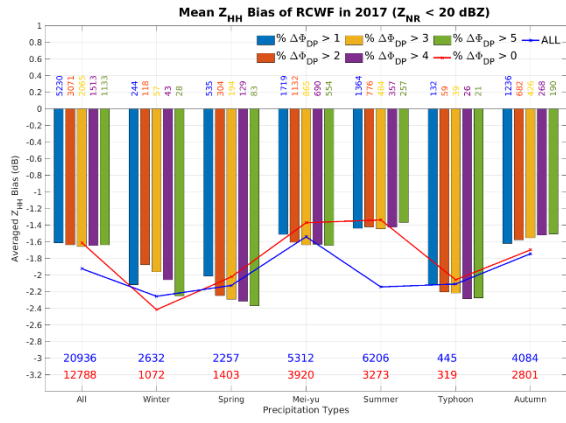


Fig. 5. The averaged biases of different percentage threshold (0-5%) of the observed $\Delta\Phi_{DP}$ volume coverage for seven different precipitation types when $Z_{NR} < 20$ dBZ. The mean Z_{HH} biases are showed in the constraints of $5^\circ < \Delta\Phi_{DP} < 30^\circ$ and $EL < 5^\circ$ except for the All (blue line). The number digits represent the number data that available with the different conditions.

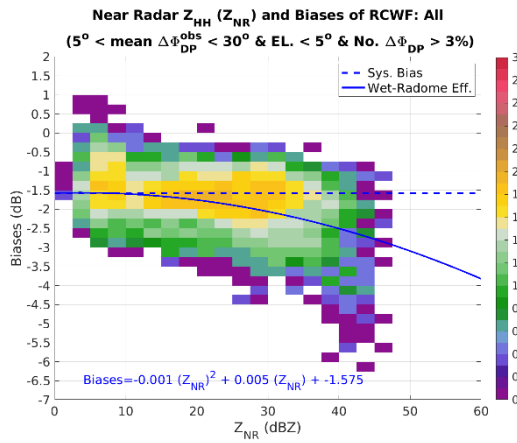


Fig. 6. The number density distribution of the Z_{NR} and averaged biases with the constraints of observed $\Delta\Phi_{DP}$, EL , and data volume coverage.

The mean Z_{HH} biases showed reasonably well and stabilize after applied the constraints of observed $\Delta\Phi_{DP}$, elevation angles, and the data volume coverage that larger than 3% (Fig. 5). The number density distribution of the Z_{NR} and biases in volume scan are also analyzed in this study, as shown in Fig. 6. It showed clearly that the biases are uniform and moved downward when Z_{NR} larger than 20 dBZ. A fitted quadratic polynomial equation is proposed to investigate the estimation of system bias and WRE, as shown in Fig. 6. This quadratic polynomial equation has shown can simultaneously obtain the systematic biases (-1.58 dB) and WRE using Z_{NR} . Fig. 3 also showed that the systematic bias is \sim

1.66 dB when $Z_{NR} < 20$ dBZ, which have a good agreement with Fig. 6.

4. Conclusions

In this study, the long-term assessment of Z_{HH} biases are analyzed from an operational S-band dual-polarization radar by accurately calibrating the Z_{HH} and Z_{DR} measurements. The Z_{HH} biases are determined by using the self-consistency constraint between K_{DP} and Z_{HH} from January 1, 2017 to December 31, 2017. The averaged Z_{HH} bias is ~ -1.6 dB and the biases (systematic, attenuation and WRE) varies from -6.33 dB to 0.75 dB. However, the ranges of the biases are reduced to -3.50 – 0.75 dB with the constraint of Z_{NR} less than 20 dBZ. This study indicates that the analysis based on the rainfall comparison shows evidently that the self-consistency method is an efficient correction of the effects introduced by a wet-radome.

References

- Atlas, D., Banks, H.C., 1951: "The Interpretation of Microwave Reflections from Rainfall", *J. Meteorol.* 8, 271–282.
- Aydin, K., Zhao, Y., Seliga, T.A., 1989: "Rain-induced attenuation effects on C-band dual-polarization meteorological radars", *IEEE Trans. Geosci. Remote Sens.* 27,57–66.
- Battan, L.J., 1973: *Radar observations of the atmosphere*, University of Chicago Press, Chicago.
- Berne, A., 2005: "A stochastic model of range profiles of raindrop size distributions: Application to radar attenuation correction", *Geophys. Res. Lett.* 32,L10803.
- Bringi, V.N., Chandrasekar, V., Balakrishnan, N., Zrnić, D.S., 1990: "An Examination of Propagation Effects in Rainfall on Radar Measurements at Microwave Frequencies", *J. Atmos. Ocean Technol.* 7,829–840.
- Bringi, V.N.N., Keenan, T.D., Chandrasekar, V., 2001: "Correcting C-band radar reflectivity and differential reflectivity data for rain attenuation: a self-consistent method with constraints", *IEEE Trans. Geosci. Remote Sens.* 39,1906–1915.
- Carey, L.D., Rutledge, S.A., Ahijevych, D.A., Keenan, T.D., 2000: "Correcting Propagation Effects in C-Band Polarimetric Radar Observations of Tropical Convection Using Differential Propagation Phase", *J. Appl. Meteorol.* 39,1405–1433.
- Chang, W.-Y., Vivekanandan, J., Chen Wang, T.-C., 2014: "Estimation of X-Band Polarimetric Radar Attenuation and Measurement Uncertainty Using a Variational

- Method", *J. Appl. Meteorol. Climatol.* 53,1099–1119.
- Chen, J.-Y., Chang, W.-Y., Chen Wang, T.-C., 2017: "Comparison of Quantitative Precipitation Estimation in Northern Taiwan Using S- and C-band Dual-Polarimetric Radars", *大氣科學* 45,57–81.
- Goddard, J.W.F., Tan, J., Thurai, M., 1994: "Technique for calibration of meteorological radars using differential phase", *Electron Lett.* 30,166–167.
- Gorgucci, E., Baldini, L., 2007: "Attenuation and Differential Attenuation Correction of C-Band Radar Observations Using a Fully Self-Consistent Methodology", *IEEE Geosci. Remote Sens. Lett.* 4,326–330.
- Gorgucci, E., Scarchilli, G., Chandrasekar, V., 1996: "Error structure of radar rainfall measurement at C-band frequencies with dual polarization algorithm for attenuation correction", *J. Geophys. Res., Atmos.* 101,26461–26471.
- Gorgucci, E., Scarchilli, G., Chandrasekar, V., Meischner, P.F., Hagen, M., 1998: "Intercomparison of Techniques to Correct for Attenuation of C-Band Weather Radar Signals", *J. Appl. Meteorol.* 37,845–853.
- Gunn, K.L.S., East, T.W.R., 1954: "The microwave properties of precipitation particles", *Q. J. R. Meteorol. Soc.* 80,522–545.
- Hitschfeld, W., Bordan, J., 1954: "Errors Inherent in the Radar Measurement of Rainfall at Attenuating Wavelengths", *J. Meteorol.* 11,58–67.
- Holt, A.R., 1988: "Extraction of differential propagation phase from data from S-band circularly polarised radars", *Electron Lett.* 24,1241.
- Keat, W.J., Westbrook, C.D., Illingworth, A.J., 2016: "High-Precision Measurements of the Copolar Correlation Coefficient: Non-Gaussian Errors and Retrieval of the Dispersion Parameter μ in Rainfall", *J. Appl. Meteorol. Climatol.* 55,1615–1632.
- Keenan, T.D., Carey, L.D., Zrnić, D.S., May, P.T., 2001: "Sensitivity of 5-cm Wavelength Polarimetric Radar Variables to Raindrop Axial Ratio and Drop Size Distribution", *J. Appl. Meteorol.* 40,526–545.
- Kim, D.-S., Maki, M., Lee, D.-I., 2010: "Retrieval of Three-Dimensional Raindrop Size Distribution Using X-Band Polarimetric Radar Data", *J. Atmos. Ocean Technol.* 27,1265–1285.
- Kim, D.-S., Maki, M., Lee, D.-I., 2008: "Correction of X-band radar reflectivity and differential reflectivity for rain attenuation using differential phase", *Atmos. Res.* 90,1–9.
- Kwon, S., Lee, G., Kim, G., 2015: "Rainfall Estimation from an Operational S-Band Dual-Polarization Radar: Effect of Radar Calibration", *J. Meteorol. Soc. Japan Ser II* 93,65–79.
- Liu, L., Bringi, V.N., Chandrasekar, V., Mueller, E.A., Mudukutore, A., 1994: "Analysis of the Copolar Correlation Coefficient between Horizontal and Vertical Polarizations", *J. Atmos. Ocean Technol.* 11,950–963.
- Oh, Y.-A., Lee, D.-H., Jung, S.-H., Nam, K.-Y., Lee, G.-W., 2016: "Attenuation Correction Effects in Rainfall Estimation at X-Band Dual-Polarization Radar: Evaluation with a Dense Rain Gauge Network", *Adv. Meteorol.* 2016,1–20.
- Park, H.S., Ryzhkov, A.V., Zrnić, D.S., Kim, K.-E., 2009: "The Hydrometeor Classification Algorithm for the Polarimetric WSR-88D: Description and Application to an MCS", *Weather Forecast* 24,730–748.
- Park, S.-G., Bringi, V.N., Chandrasekar, V., Maki, M., Iwanami, K., 2005: "Correction of Radar Reflectivity and Differential Reflectivity for Rain Attenuation at X Band. Part I: Theoretical and Empirical Basis", *J. Atmos. Ocean Technol.* 22,1621–1632.
- Ryde, J.W., 1946: The attenuation and radar echoes produced at centimetre wave-lengths by various meteorological phenomena, In: *Meteorological Factors in Radio Wave Propagation*, The Physical Society, The Royal Institution, London, pp 169–188.
- Ryzhkov, A.V., Zrnić, D.S., 1996: "Assessment of Rainfall Measurement That Uses Specific Differential Phase", *J. Appl. Meteorol.* 35,2080–2090.
- Ryzhkov, A.V., Giangrande, S.E., Melnikov, V.M., Schuur, T.J., 2005: "Calibration Issues of Dual-Polarization Radar Measurements", *J. Atmos. Ocean Technol.* 22,1138–1155.
- Scarchilli, G., Gorgucci, V., Chandrasekar, V., Dobaie, A., 1996: "Self-consistency of polarization diversity measurement of rainfall", *IEEE Trans. Geosci. Remote Sens.* 34,22–26.
- Tang, L., Zhang, J., Langston, C., Krause, J., Howard, K., Lakshmanan, V., 2014: "A Physically Based Precipitation–Nonprecipitation Radar Echo Classifier Using Polarimetric and Environmental Data in a Real-Time National System", *Weather Forecast* 29,106–119.
- Vivekanandan, J., Zhang, G., Ellis, S.M., Rajopadhyaya, D., Avery, S.K., 2003: "Radar reflectivity calibration using differential propagation phase measurement", *Radio Sci.* 38,14-1-14-14.
- Zrnić, D.S., Ryzhkov, A., 1996: "Advantages of Rain Measurements Using Specific Differential Phase", *J. Atmos. Ocean Technol.* 13,454–464.